

Nail Suleimanov<sup>a,b</sup>, Sergey Khantimerov<sup>a</sup>, Krzysztof Kierzek<sup>c</sup>, Vladimir Shustov<sup>a</sup>, Ranis Garipov<sup>a</sup>, Ranis Fatukhov<sup>a</sup>, Vadim Matukhin<sup>b</sup>

<sup>a</sup>Zavoisky Physical-Technical Institute, FRC Kazan Scientific Center of RAS, Kazan, Russia

<sup>b</sup>Kazan State Power Engineering University, Kazan, Russia

<sup>c</sup>Wroclaw University of Science and Technology, Wroclaw, Poland

# Structural and electrochemical properties of lithiated conical carbon nanotubes as anode materials for lithium ion accumulating systems

Interaction of conical carbon nanotubes with lithium during their electrochemical treatment was studied by galvanostatic measurements. The presence of reversible and irreversible reactions during the Li insertion into conical carbon nanotubes was established. The structural changes occurring in the conical walls of the conical carbon nanotubes in consequence of the lithium intercalation were investigated by using X-ray diffraction. The results obtained show that the lithiation of conical carbon nanotubes is partially reversible and leads to a change in the diffraction peak profile ( $2\theta = 26^\circ$ ) corresponding to the interplanar distance in conical carbon nanotubes. Such changes are associated with the lithium insertion into the interplanar spaces of conical carbon nanotubes.

**Keywords:** Li-ion batteries; Anode material; Conical carbon nanotubes; Electrochemical properties

## 1. Introduction

At the present time intense investigations are being carried out aimed on the development of new generation of Li ion batteries with high energy capacity and life time [1–3]. The search for new anode and cathode materials leading to improved electrochemical properties and economical lithium ion batteries is an ongoing pursuit. Most commercially available lithium batteries have  $\text{LiCoO}_2$  as the cathode material [4, 5]. Since the cobalt oxide cathode is expensive and toxic, a variety of other materials [6] are being extensively studied as possible replacements to make lithium ion batteries environmentally benign and cost effective. In spite of the fact that strong attention is devoted to the investigation of cathode materials, it is difficult to expect a breakthrough in this field without a comprehensive approach based on the development of new materials for the anode of Li accumulators [7, 8]. The energy capacity of accumulating systems based on the use of lithium or sodium as the “working ion” is determined by the amount of lithium ions which are able to move reversibly between cathode and anode in the process of charging/discharging of Li-ion batteries. Along with high content of lithium in the cathode material, the high effective surface of the anode

material is crucial for Li-ion batteries. It requires new materials with high absorption capacity and reversible properties in relation to the Li ions. Of all the family of anode materials studied, carbon-based anodes [9–11] are considered leading candidates due to their low working voltage with respect to lithium, high coulombic efficiency, ease in preparation in various forms, and low environmental impact.

Traditionally, graphite is commonly used as an anode material for Li-ion batteries [12, 13]. However, the capacity of Li-ion batteries based on graphite as an anode material is limited, since the intercalation of lithium into graphite involves one lithium atom per six carbon atoms, i.e.,  $\text{LiC}_6$ , leading to a theoretical specific capacity of  $372 \text{ mA h g}^{-1}$  and an observed capacity of  $280\text{--}330 \text{ mA h g}^{-1}$ , depending on the type of graphite used [14]. Carbon nanotubes (CNTs), an allotrope of graphite, have been reported to show much improved lithium capacity compared to graphite due to their unique structures and properties. Multi-walled carbon nanotubes (MWCNTs) consisting of concentric graphite spheres with interlayer distance of 0.34 nanometers and lengths of tens of micrometers are considered as a medium similar to graphite from the point of view of Li intercalation but with essentially higher effective surface area [15, 16]. Indeed, the high effective surface area of MWCNTs both external and internal ones gives the possibility to absorb a high amount of Li. At the same time, the micrometer lengths can essentially impede the filling of internal space of carbon nanotubes by Li ions. This explains, in particular, the results where the lithium absorption was increased by the shortening of multiwalled carbon nanotubes by means of ball milling [17]. In this connection, great attention is given to conical carbon nanotubes (cCNTs) [18]. A characteristic feature of cCNTs is that their walls consist of single graphite planes forming the array of conical segments with open ends and hundred of nanometers in length [19, 20]. Thus, there is the possibility of adsorption of light elements by the surface of carbon nanotubes, as well as the possibility of their intercalation into the interplanar space of conical segments [21]. A recent paper reported on the synthesis of cCNTs decorated with silicon by magnetron sputtering. The prototypes obtained were used as an anode of a lithium ion battery without the use of binding conductive additives and showed a high effective capacity of about 2000 mAh per gram of active substance

[22]. Therefore, conical carbon nanotubes seem to be a good candidate for anodes of lithium-ion batteries.

The purpose of this work was to study the process of electrochemical lithium intercalation into the cCNTs and to investigate structural properties of the material at different lithiation states.

## 2. Experimental procedure

The approach realized in this paper is based on the development and investigation of anode electrode material consisting of conical CNTs grown directly on metallic nickel plate. This approach does not need any binders or other additional substances to fabricate the anode electrode. cCNTs were grown on specially treated Ni plates by thermal chemical vapor deposition (CVD). In these experiments granular polyethylene was pyrolysed at suitable temperatures and the products then passed over a nickel catalyst using helium as a buffer gas. The catalyst used was a nickel plate located inside a quartz reactor. The most representative conditions were as follows: total pressure 4–5 atm., reaction temperatures ranging from 500–600 °C, reaction time 15–20 min. The average surface loading of cCNT was about 1.6 mg cm<sup>-2</sup> (one side covering). These nanotubes (Fig. 1) are several microns in length, with outer diameters ranging between 40 and 50 nm and inner channels varying between 9 and 20 nm. The fringe spacing is 0.34 nm. A characteristic feature of these tubes is their conical structure formed by the open graphite planes.

Electrochemical lithium insertion/deinsertion was performed in coin-type cells (CR2032, Honsen Corp., Japan), which were assembled with the nickel plate covered with conical CNT as anode and a metallic lithium foil as cathode and reference electrode. The electrolyte used was a 1 M solution of lithium hexafluorophosphate (LiPF<sub>6</sub>) in a 1:1 mixture of EC (ethylene carbonate) and DMC (dimethyl carbonate). A glass microfiber separator (Whatman, thickness of 420 μm), wetted with the electrolyte, was sandwiched between the anode and Li metal foil. All the operations for assembling the electrochemical cell were carried

out in an argon filled glove-box (MBraun, Germany). The cells were investigated at ambient temperature by galvanostatic cycling using a VSP (Biologic, France) multichannel generator. The initial discharge (lithium insertion) test was carried out at constant current -0.4 mA down to a potential of 0.005 V vs. Li. The subsequent charge test (lithium deinsertion) started at a constant current of 0.4 mA and lasted until the potential reached 2 V. The cycles were repeated 50 times. The final sweep was ended at potential of 0.005 V (fully lithiated) or 2 V (totally delithiated). Then, the cell was disassembled in the glove-box. The substrate was washed with DMC and subjected to X-ray diffraction (XRD) analysis.

X-ray diffraction experiments on initial (non-treated electrochemically) and lithiated/delithiated samples were carried out using a DRON-7 diffractometer in the Bragg-Brentano geometry ( $\theta$ - $2\theta$ ) with Cu-K $\alpha$  radiation ( $\beta$ -filter mode, 40 kV/20 mA). Nickel foil annealed in a hydrogen atmosphere was used to calibrate the instrumental function. The diffraction pattern was scanned three times in the range of angles from 5° to 45° with increments of 0.02°. The three measurements' data were summed. The range of angles was chosen to capture the reflections of graphite (002) at  $2\theta = 26^\circ$  and nickel (111) at  $2\theta = 44^\circ$ . This peak of Ni (111) was used as the internal standard (lattice distance was equal to 3.5238 Å). The peak position of graphite (002) was determined comparatively to that of Ni (111). XRD line-profile analysis was based on the approach developed in Rietveld method [23]. As it was expected that the lithium intercalation would create certain crystal imperfections and microstrains in conical segments of carbon nanotubes, the determination of crystal size and microstrain values was carried out in the frame of single-line method [23, 24] where the diffraction line is described as a combination of a Gaussian and a Lorentzian components corresponding to the microstrain and finite crystalline size contributions, respectively. Spectrum processing was performed using the MAUD (materials analysis using diffraction) program v2.33 [25].

## 3. Results and discussion

Typical lithium charging/discharging curves are shown in Fig. 2. The results show that intercalation/deintercalation of lithium ions on cCNTs in the 2<sup>nd</sup> and subsequent cycles is reversible. However, the applied potential is insufficient for the entire Li deintercalation from conical carbon nanotubes. The reversible capacity ( $C_{rev}$ ) can be defined as the first charge capacity while the irreversible capacity ( $C_{irr}$ ) is defined as the difference between the first discharge and charge capacities. As one can see, the initial potential for the conical CNTs decreased rapidly and formed a plateau at 0.75 V when a current was applied to insert Li in the first discharge. The phenomenon was observed only in the first discharge process and seems to be associated with the reduction reaction of the surface groups of cCNTs with Li ions and formation of solid electrolyte interface (SEI) layer [26].

Differential capacity ( $dQ/dV$ ) vs. potential curves drawn using the data in Fig. 2 are presented in Fig. 3. The first discharge derivative curve showed a peak corresponding to insertion of Li ions, but no peak was observed in the second discharge derivative curves. The peak appeared in the first discharge derivative curve, corresponding to the voltage

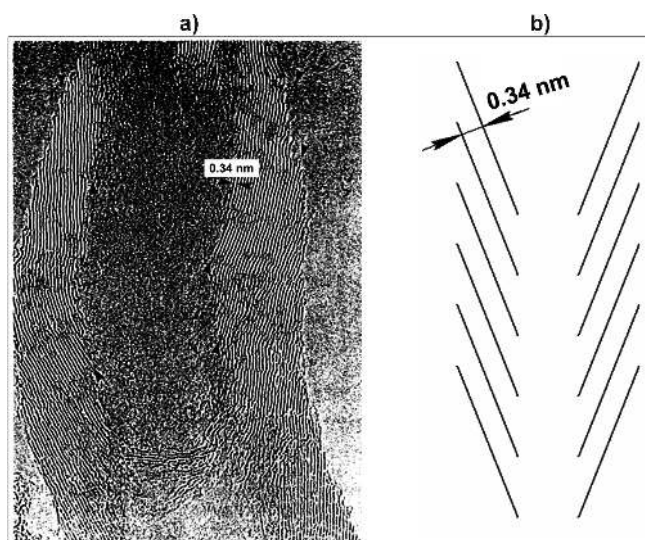


Fig. 1. (a) TEM image [19], and (b) schematic view of a fragment of conical carbon nanotube.

plateau in the discharge curve, is due presumably to an irreversible reaction in the Li insertion into cCNTs [27, 28]. In the first discharge, the decomposition of electrolyte and the formation of solid electrolyte interface on the surface of cCNTs result in the large  $C_{irr}$  in carbon nanotubes [26, 29, 30].

The X-ray diffraction spectra for the initial, lithiated and delithiated samples are shown in Figs. 4, 5 and 6, respectively. As one can see, a distinct diffraction peak which is characterized by broad wings is observed for all investigated samples around  $2\theta = 26^\circ$ . This indicates that the observed X-ray diffraction line consists of the narrow and broad patterns which both are associated with diffraction of the 002 hexagonal graphite planes. It is known that the process of carbon nanotube synthesis by means of CVD technique is always accompanied by the formation of a certain amount of graphite species (see, for example [31]).

To describe the peak profile, its approximating curve was divided into constituent parts. It was determined that the use of two components is sufficient for a thorough description of the profile (the calculated lines 5 and 6 which are indicated as Graphite 1 and Graphite 2). Comparing the table data for the crystal structure of graphite [32] and the lattice parameters of Graphite 1 (Table 1), allowed us to ascribe the Graphite 1 to the graphite species and Graphite 2 to carbon nanotubes. In addition, the narrow diffraction line of Graphite 1 indicates that this phase is better crystallized, that is typical for the graphite rather than carbon nanotubes.

This can be seen from the dimensions of crystallite sizes (cryst. size) specified in Table 2.

The XRD patterns of the lithiated and delithiated nanotubes show both the Bragg peaks of the initial conical carbon nanotubes and a new set of reflections. It follows from the analysis that these reflections correspond to lithium carbonate  $\text{Li}_2\text{CO}_3$ . Indeed, the solid electrolyte interface is formed as the result of electrochemical reduction of electrolyte on the surface of negative carbon electrode. While the SEI has been reported to be a complex mixture of compounds, it contains mainly lithium carbonate ( $\text{Li}_2\text{CO}_3$ ) and the metallorganic compounds: lithium ethylene dicarbonate ( $\text{CH}_2\text{OCO}_2\text{Li}$ )<sub>2</sub> and lithium alkyl carbonates ( $\text{ROCO}_2\text{Li}$ ) [33].

The quantitative ratios of obtained phases and crystallite-size values for the samples studied are presented in Table 2. As can be seen, the electrochemical delitiation process leads to the decreasing of the  $\text{Li}_2\text{CO}_3$  phase with the simultaneous rise of the graphite and carbon nanotube components that can be connected with the  $\text{Li}_2\text{CO}_3$  decomposition in the electrochemical delitiation process. It was recently reported that  $\text{Li}_2\text{CO}_3$  can be electrochemically decomposed to  $\text{Li}_2\text{O}$  and  $\text{CO}_2$  in the presence of NiO [34].

It was found that the electrochemical lithium intercalation into the conical carbon nanotubes leads to change in the diffraction peak profile ( $2\theta = 26^\circ$ ) corresponding to the interplanar distance in the cCNTs. As can be seen from Table 1 the lithiation increases the cell length ( $c$ ), which indicates the structural changes occurring in the conical seg-

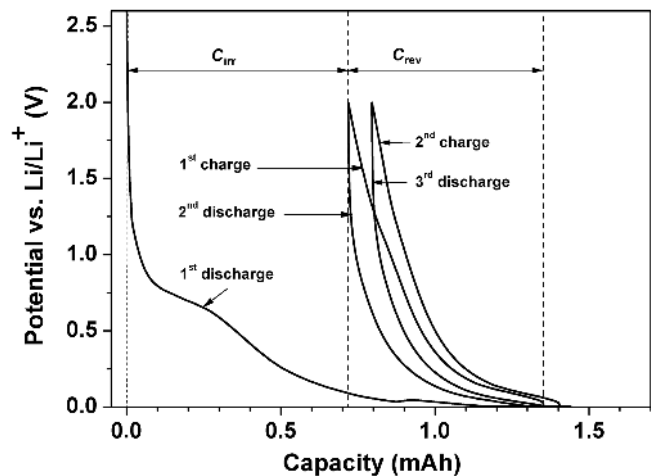


Fig. 2. Typical charge/discharge curves of a prototype electrode based on nickel plates and conical carbon nanotubes grown on its surface layers.

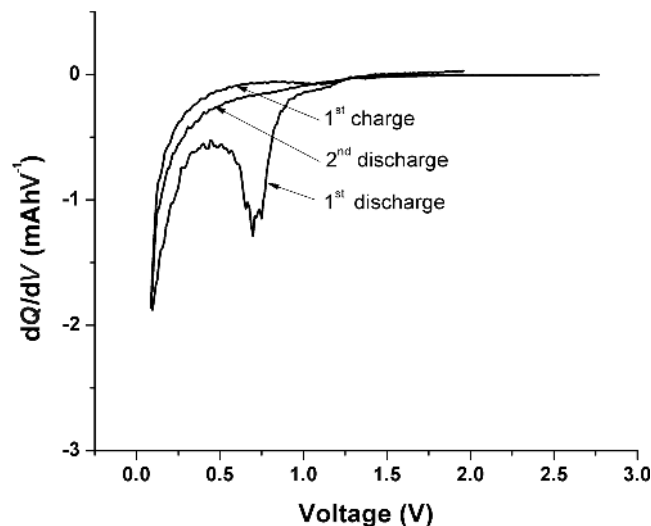


Fig. 3. Differential capacity ( $dQ/dV$ ) vs. potential curves of the first discharge/charge and the second discharge curves.

Table 1. Structural properties of initial, lithiated and delithiated cCNTs.

Sample	Graphite 1		Graphite 2	
	cell length ( $c$ ) (Å)	microstrain (%)	cell length ( $c$ ) (Å)	microstrain (%)
Initial	$6.817 \pm 0.005$	$2.41 \pm 0.15$	$7.016 \pm 0.005$	$0.856 \pm 0.15$
Lithiated	$6.828 \pm 0.005$	$2.55 \pm 0.15$	$7.231 \pm 0.005$	$1.55 \pm 0.15$
Delithiated	$6.821 \pm 0.005$	$2.42 \pm 0.15$	$7.135 \pm 0.005$	$0.97 \pm 0.15$

ments of carbon nanotubes caused by the intercalation of lithium into the interplanar space of conical CNTs. It is interesting to note that after delithiation the cell parameter decreases but is still large in comparison with the initial sample. This may indicate that microstrains are accumulated in the sample during lithiation/delithiation. This is evidenced by the fact that the microstrains increased almost by 2 times in the lithiated conical carbon nanotubes compared with the initial samples.

#### 4. Conclusions

Among various types of carbon nanotubes much attention is drawn to conical CNTs. A characteristic feature of this type of CNTs is that their walls are constituted from conical segments with open edges. Such opened structure of cCNTs can help to improve the capacity and electrical transport in CNT-based Li ion batteries. Conical CNTs were synthesized directly on metallic nickel plate by thermal CVD. The investigation of electrochemical interaction of lithium with conical CNTs was performed. The results show that the discharge/charge curve (intercalation/deintercalation of lithium ions) of conical carbon nanotubes is reversible. At the same time, the applied potential is insufficient for Li entire deintercalation corresponding to the presence of reversible and irreversible reactions during the Li insertion into conical carbon nanotubes. The X-ray diffraction method revealed that the electrochemical lithiation leads to a change in the diffraction peak ( $2\theta = 26^\circ$ ) profile corresponding to the interplanar distance in the CNTs. It is also found that the microstrains in conical segments of carbon tubes increased significantly after lithiation. Such changes were associated with the lithium insertion into the interplanar spaces of conical CNTs. Furthermore, the delithiation led to a decrease in the interplanar distance, however, the cell length ( $c$ ) did not return to its initial value. This indicates that microstrains are accumulating in the samples investigated during lithiation/delithiation processes.

Table 2. Composition and crystallite-size values of initial, lithiated and delithiated cCNTs.

Sample	atom %	cryst. size (Å)
Initial		
Nickel	0.0868	5172.71
Graphite 1	0.2203	1388.23
Graphite 2	0.6929	10.6919
Lithiated		
Nickel	0.1026	6620.38
Graphite 1	0.1683	1421.89
Graphite 2	0.4100	19.03
Li <sub>2</sub> CO <sub>3</sub>	0.3191	220.46
Delithiated		
Nickel	0.0612	6045.12
Graphite 1	0.2086	1408.30
Graphite 2	0.5581	12.86
Li <sub>2</sub> CO <sub>3</sub>	0.1721	198.62

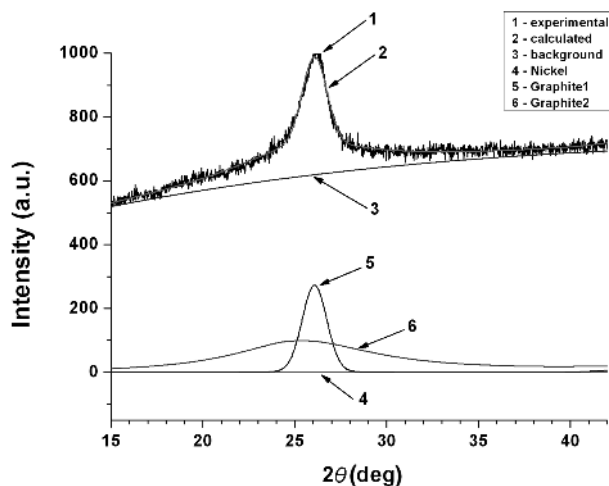


Fig. 4. X-ray diffraction pattern of the initial sample of conical CNTs. The lower part of the figure shows the spectra of the experimental line components.

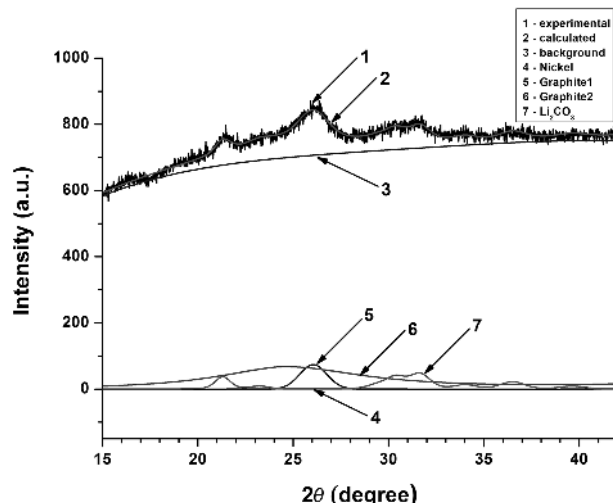


Fig. 5. X-ray diffraction pattern of the lithiated sample of conical CNTs. The lower part of the figure shows the spectra of the experimental line components.

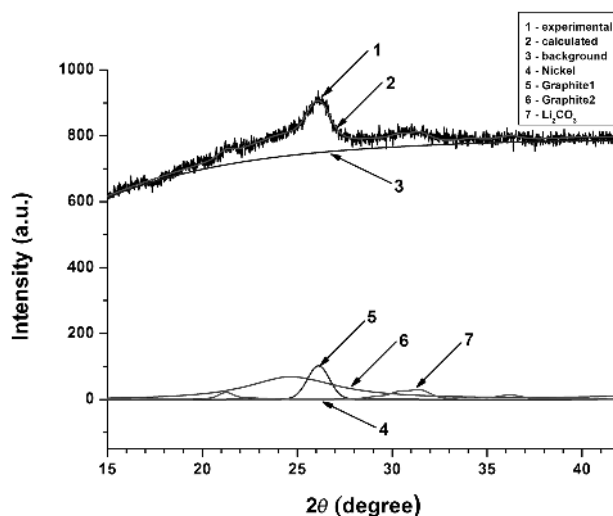


Fig. 6. X-ray diffraction pattern of the delithiated sample of conical CNTs. The lower part of the figure shows the spectra of the experimental line components.

This work was done within the framework of fundamental research AAAA-A18-118041760011-2 of FRC Kazan Scientific Center of RAS and partially financed by a statutory activity subsidy from the Polish Ministry of Science and Higher Education for the Faculty of Chemistry of Wrocław University of Science and Technology.

## References

- [1] J.B. Goodenough, K.-S. Park: *J. Am. Chem. Soc.* 135 (2013) 1167. PMID:23294028; DOI:10.1021/ja3091438
- [2] Da Deng: *Energy Sci. Eng.* 3 (2015) 385. DOI:10.1002/ese3.95
- [3] E.B. George: *J. Electrochem. Soc.* 164 (2017) 5019. DOI.org/10.1149/2.0251701jes. DOI:10.1149/2.0091707jes
- [4] J. Li, R. Zhao, X. He, H. Liu: *Ionics* 15 (2009) 111. DOI:10.1007/s11581-008-0238-8
- [5] J.W. Fergus: *J. Power Sources* 195 (2010) 939. DOI:10.1016/j.jpowsour.2009.08.089
- [6] J. Xu, S. Dou, H. Liu, L. Dai: *Nano Energy* 2 (2013) 439. DOI:10.1016/j.nanoen.2013.05.013
- [7] S. Goriparty, E. Miele, F. De Angelis, E. Di Fabrizio, R. Proietti Zaccaria, C. Capiglia: *J. Power Sources* 257 (2014) 421. DOI:10.1016/j.jpowsour.2013.11.103
- [8] N. Loeffler, D. Bresser, S. Passerini: *Johnson Matthey Technol. Rev.* 59 (2015) 34. DOI:10.1595/205651314x685824
- [9] R. Fong, U.V. Sacken, J.R. Dahn: *J. Electrochem. Soc.* 137 (1990) 2009. DOI:10.1149/1.2086855
- [10] Y.P. Wu, E. Rahm, R. Holze: *J. Power Sources* 114 (2003) 228. DOI:10.1016/S0378-7753(02)00596-7
- [11] C. Jiang, E. Hosono, H. Zhou: *Nano Today* 1 (2006) 28. DOI:10.1016/S1748-0132(06)70114-1
- [12] T. Ohzuku, Y. Iwakoshi, K. Sawai: *J. Electrochem. Soc.* 140 (1993) 2490. DOI:10.1149/1.2220849
- [13] R.M. Humana, M.G. Ortiz, J.E. Thomas, S.G. Real, M. Sedlarikova, J. Vondrak, A. Visintin: *ECS Trans.* 63 (2014) 1053. DOI:10.1007/s10008-015-3004-7
- [14] Z.G. Yang, J.L. Zhang, M.C.W. Kintner-Meyer, X.C. Lu, D. Choi, J.P. Lemmon, J. Liu: *Chem. Rev.* 111 (2011) 3577. PMID:21375330; DOI:10.1021/cr100290v
- [15] Charles de las C., W. Li: *J. Power Sources* 208 (2012) 74. DOI:10.1016/j.jpowsour.2012.02.013
- [16] J.L. Brian, D.C. Cory, P.R. Ryne: *J. Mater. Res.* 25 (2010) 1636. DOI:10.1557/JMR.2010.0209
- [17] R.A. DiLeo, A. Castiglia, M.J. Ganter, R.E. Rogers, C.D. Cress, R.P. Raffaele, B.J. Landi: *ACS Nano* 4 (2010) 6121. PMID:20857949; DOI:10.1021/nn1018494
- [18] Z. Xiong, Y.S. Yun, H.-J. Jin: *Materials* 6 (2013) 1138. PMID:28809361; DOI:10.3390/ma6031138
- [19] E.F. Kukovitsky, L.A. Chernozatonskii, S.G. L'vov, N.N. Melnik: *Chem. Phys. Lett.* 266 (1997) 323. DOI:10.1016/S0009-2614(97)00020-1
- [20] E.F. Kukovitsky, S.G. L'vov, N.A. Sainov, V.A. Shustov, L.A. Chernozatonskii: *Chem. Phys. Lett.* 355 (2002) 497. DOI:10.1016/S0009-2614(02)00283-X
- [21] S.M. Khantimerov, V.A. Shustov, N.V. Kurbatova, E.F. Kukovitsky, V.L. Matukhin, Y.A. Sakhratov, N.M. Suleimanov: *Appl. Phys. A.* 113 (2013) 597. DOI:10.1007/s00339-013-7697-0
- [22] W. Wang, I. Ruiz, K. Ahmed, H.H. Bay, A.S. George, J. Wang, J. Butler, M. Ozkan, C.S. Ozkan: *Small* 10 (2014) 3389. DOI:10.1002/smll.201400088
- [23] *The Rietveld Method*, ed. by R.A. Young (International Union of Crystallography, Oxford, University Press, 1995), 312 p.

- [24] E. Mittemeijer, U. Welzel: *Z. Kristallogr.* 223 (2008) 552. DOI:10.1524/zkri.2008.1213
- [25] L. Lutterotti, M. Bortolotti, G. Ischia, H.-R. Wenk: *Z. Kristallogr. Suppl.* 26 (2007) 125. DOI:10.1524/zksu.2007.suppl\_26.125
- [26] E. Frackowiak, S. Gautier, H. Gaucher, S. Bonnamy, F. Béguin: *Carbon* 37 (1999) 61. DOI:10.1016/S0008-6223(98)00187-0
- [27] Z.H. Yang, H.Q. Wu: *Solid State Ionics* 143 (2001) 173. DOI:10.1016/S0167-2738(01)00852-9
- [28] W. Xing, J.R. Dahn: *J. Electrochem. Soc.* 144 (1997) 1195. DOI:10.1149/1.1837572
- [29] G.T. Wu, C.S. Wang, X.B. Zhang, H.S. Yang, Z.F. Qi, P.M. He, W.Z. Li: *J. Electrochem. Soc.* 146 (1999) 1696. DOI:10.1149/1.1391828
- [30] J.Y. Eom, H.S. Kwon, J. Liu, O. Zhou: *Carbon* 42 (2004) 2589. DOI:10.1016/j.carbon.2004.05.039
- [31] A. Szabó, C. Perri, A. Csató, G. Giordano, D. Vuono, J. Nagy: *Materials* 3 (2010) 3092. DOI:10.3390/ma3053092
- [32] R.W.G. Wyckoff: *Crystal Structures*, sec. ed., vol. 1, Interscience Publishers, New York (1963).
- [33] B.S. Parimalam, A.D. MacIntosh, R. Kadam, B.L. Lucht: *J. Phys. Chem. C* 121 (2017) 22733. DOI:10.1021/acs.jpcc.7b08433
- [34] C. Ling, R.G. Zhang, K. Takechi, F. Mizuno: *J. Phys. Chem. C* 118 (2014) 26591–26598. DOI:10.1021/jp5093306

(Received September 6, 2018; accepted April 2, 2019; online since August 2, 2019)

## Correspondence address

Sergey Khantimerov, PhD  
Senior Fellow  
Zavoisky Physical-Technical Institute  
FRC Kazan Scientific Center of RAS  
Kazan  
Russia  
Tel.: +7 843 2319123 (add.5)  
Fax: +7 843 2725075.  
E-mail: khantim@mail.ru

## Bibliography

DOI 10.3139/146.111821  
*Int. J. Mater. Res. (formerly Z. Metallkd.)*  
110 (2019) 10; page 931–935  
© Carl Hanser Verlag GmbH & Co. KG  
ISSN 1862-5282